

Reflection electron-energy-loss investigation of the electronic and structural properties of palladium

G. Chiarello, E. Colavita, and M. De Crescenzi

*Dipartimento di Fisica, Università degli Studi della Calabria, Arcavacata di Rende, Cosenza, Italy
and Gruppo Nazionale di Struttura della Materia, Cosenza, Italy*

S. Nannarone

*Dipartimento di Fisica, Università degli Studi di Roma "La Sapienza," I-00185 Roma, Italy
and Gruppo Nazionale di Struttura della Materia, I-00185 Roma, Italy*

(Received 22 April 1983; revised manuscript received 10 November 1983)

The versatility of electron-energy-loss spectroscopy for investigating the electronic as well as the structural properties of a bulk sample is shown. The technique should be considered a powerful tool for ranging from low to high energies in the same experimental apparatus. The electronic properties of palladium are interpreted in detail within band-structure framework and confirmed through a systematic investigation of adjacent transition metals. The structural properties obtained by analyzing extended energy-loss fine structures above shallow core levels are presented in the form of the radial distribution function. These extended x-ray-absorption fine-structure-like oscillations detected above the N_{23} and M_{45} core levels of Pd support the signal interpretation scheme of the high-energy-loss range.

I. INTRODUCTION

The electronic and structural properties of palladium are studied by means of the same technique [reflection electron-energy-loss (REEL) spectroscopy (Ref. 1)] within the facilities of the same experimental apparatus. The usual optical techniques² would require different setups in order to monochromatize the electromagnetic radiation. Moreover, different procedures of sample preparation, one for each energy range, would also be necessary. Instead, the use of the REEL spectroscopy in a scattering reflection geometry³ allows us to overcome many such problems.

As it is well known, "valence" REEL spectra³ (2–30 eV) give quantitative information on the electronic properties of the sample ("optical" interband transitions and plasmons), while "core" extended energy-loss fine-structure (EELFS) spectra,^{4,5} similar to extended x-ray-absorption fine-structure (Ref. 6) (EXAFS) spectra, are related to the geometric properties of the solid (lattice parameter, coordination number, vibration frequency, etc.).

Both valence and core spectra have already been recorded in the REEL mode and successfully interpreted for a number of transition metals of the first row.^{7,8} This is the first attempt to obtain electronic and structural information on a transition metal of the second row at the same time. This should be a further test of the interpretation scheme of valence spectra within the energy-band structure framework and of core spectra within the EXAFS-like theory.⁶

The REEL spectra have been taken at several beam energies in order to distinguish between surface and volume contributions in the low-energy-loss range (2–30 eV). The structures can be interpreted in terms of a volume scatter-

ing loss function even at low primary-beam energies (as low as 50 eV). This point is supported by careful comparison with optical^{9,10} and transmission¹¹ electron-energy-loss data which are generally unaffected by surface effects and, moreover, confirmed by a phenomenological model¹² which weighs surface versus bulk scattering.

All of the observed energy-loss structures can be interpreted in terms of single-particle excitations within the Pd energy-band structure, confirming that the dipole matrix element gives the most important contribution to the inelastic scattering cross section. A straightforward conclusion is that the transverse and the longitudinal dielectric function³ of Pd can be considered to coincide, at least when the REEL experiment is performed in the reflection mode and without the angular resolution.

The analysis of the REEL oscillations above the N_{23} and M_{45} edges of palladium provides structural information in the same manner as EXAFS. Once more^{5,8} it has been shown that an accurate radial distribution function can be obtained from the REEL spectra recorded above shallow core levels.

The versatility of the REEL technique can open new research fields into solid-state and surface physics. In particular, it appears very suitable for interface problems^{13–15} where electronic and structural investigations performed *in situ* are required. The present work on pure Pd should also be considered as a preliminary step before extensive studies of Pd-semiconductor interfaces. Previous core EELFS works of chemisorption on metal surfaces^{16–18} make us confident that quantitative information can also be obtained from interface experiments.

This paper is organized as follows: In Sec. II the experimental technique is described and the results presented. In Sec. III valence REEL spectra are interpreted by using

both the Pd band-structure calculations¹⁹ which recently appeared in the literature and a systematic comparison to adjacent metals. Also the surface-to-volume scattering ratio is evaluated. In Sec. IV the core excitation region is investigated. The origin of the structures is discussed and the structural information obtained from EXAFS-like oscillations are presented. Conclusions and comments are presented in Sec. V.

II. EXPERIMENT AND RESULTS

The pure (99.9999%) polycrystalline Pd sample was cut to size ($5 \times 5 \times 2$ mm³), mechanically polished through 1- μ m alumina abrasive to obtain a specular surface, and

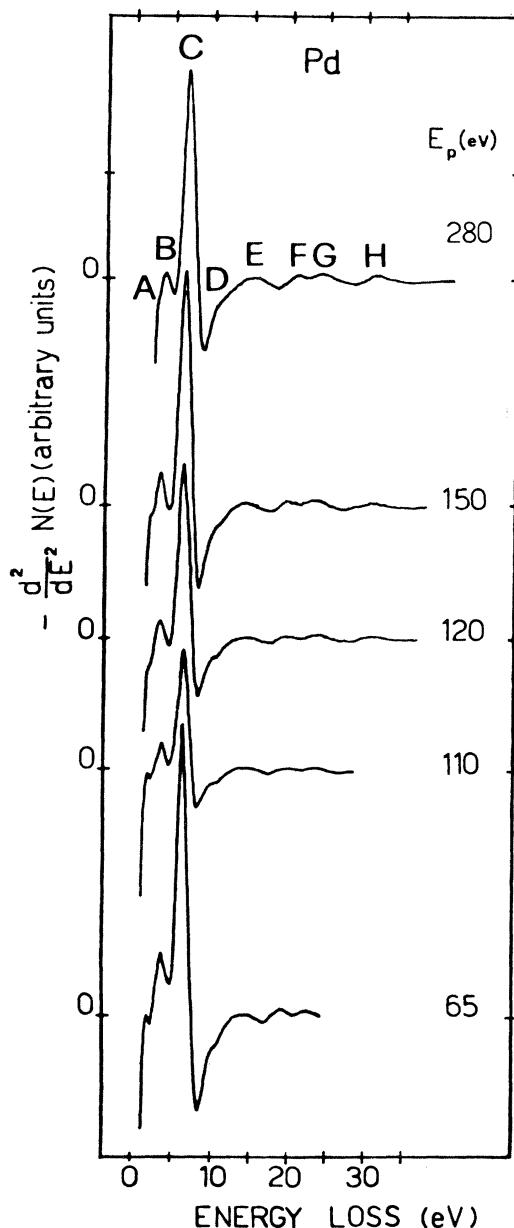


FIG. 1. Valence electron-energy-loss spectra of clean palladium taken at different primary-beam energies.

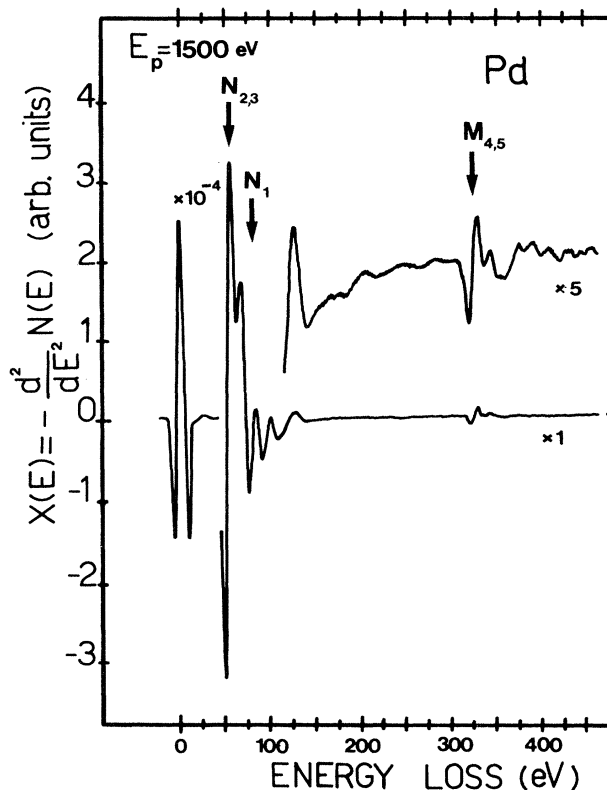


FIG. 2. Core electron-energy-loss spectrum of clean palladium taken at primary-beam energy $E_p = 1500$ eV. EXAFS above the $N_{2,3}$ and $M_{4,5}$ core levels are clearly visible.

then chemically etched to remove the cold-worked layers. The base pressure of the ultrahigh-vacuum (UHV) chamber was in the 10^{-10} -Torr range.

The UHV apparatus was equipped with an electron-gun coaxial to a Varian single-pass cylindrical-mirror analyzer (CMA) which has been driving in a first (Auger spectroscopy) and in a second- (REELS) derivative mode. The typical energy modulation was $1V_{pp}$ in the valence band and $(5-10)V_{pp}$ in the core-loss range.

Clean surfaces were obtained by cycles of ion argon bombardment by means of an Atomika ion gun with a differential pump system. The surface status was monitored by Auger spectroscopy after every cycle and Pd was assumed to be clean when the peak-to-peak ratio between Pd and contaminants (essentially oxygen, carbon and chlorine) were well below 0.5×10^{-2} . The cleanliness was also checked in a complementary way by looking at the contaminant edges in the electron-energy-loss spectra. This method is, in fact, more sensitive to low traces of contaminants than the Auger spectroscopy itself when superposition of Auger transitions occurs [i.e., KVV of carbon (~ 280 eV) and $M_{4,5}VV$ of palladium]. The surface cleanliness was monitored again after every run especially in the case of core spectra which require an integration time of about 3 sec, that means about ~ 15 min of recording time for a single spectrum.

Figure 1 shows the valence REEL spectra taken at different primary-beam energies. The structures which are labeled as B-H do not show either a position or an inten-

sity dependence on the primary-beam energy. Peak *A*, instead, changes with increasing E_p , becoming only a shoulder when $E_p = 280$ eV. However, this behavior is very likely due to the energy resolution of the analyzer which is driven in the $\Delta E/E$ constant mode. The overall shape and the energy position of the peaks are in fairly good agreement with recent electron-energy-loss measurements^{14,20} on Pd evaporated film.

In Fig. 2 the core EELFS's of Pd above N_{23} and M_{45} edges (loss energies ~ 51 and ~ 340 eV, respectively) are shown. The spectra do not display the expected anomalous M_{45} threshold delay^{21,22} due to the centrifugal potential of the $4f$ final states. Since the $d-p$ channel contributes significantly only at threshold while the $d-f$ channel gives rise to strong absorption after the f barrier is surmounted, the M_{45} absorption is expected to occur about 30–40 eV beyond the excitation edge. We observe the M_{45} edge at about 340 eV instead of 380 eV, probably because of the use of the second-derivative mode in the data acquisition. In our case, in fact, the sharp $d-p$ edge

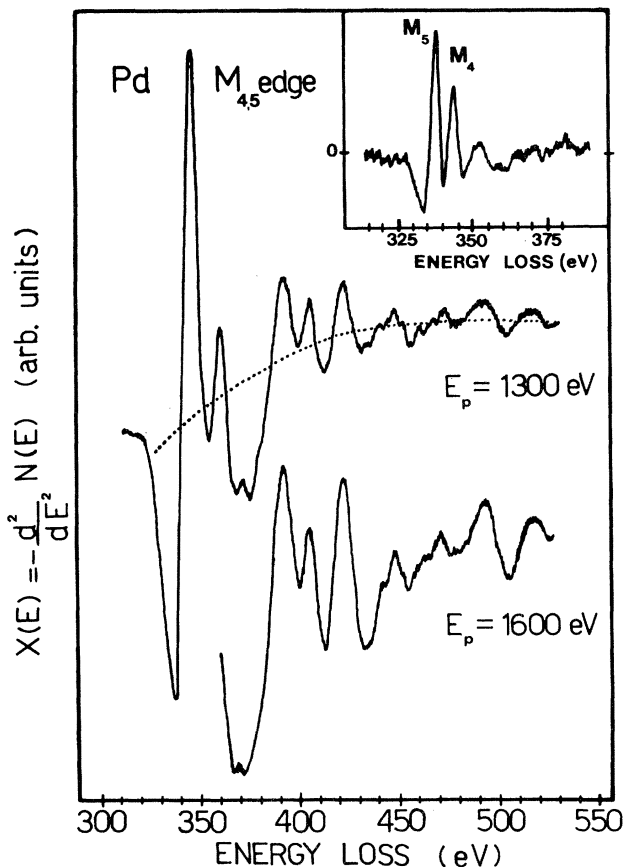


FIG. 3. Electron-energy-loss features above the M_{45} core levels taken at two different primary-beam energies. The dotted line shows the background subtraction used to extract the electron-energy-loss spectra oscillations. The deeper core levels M_{23} ($E_{M_3} \approx 532$ eV; $E_{M_2} \approx 560$ eV) restrict the integration k range of the Fourier transform at $k_{\max} = 8 \text{ \AA}^{-1}$. The inset shows the spin-orbit structure of the M_{45} edge obtained with a peak-to-peak modulation of ~ 2 V.

transition should be enhanced at the expense of the slowly varying $d-f$ absorption.

The EELFS oscillations do not show any primary-beam energy dependence when E_p is varied in the 1000–2000 eV energy range (Fig. 3), but have an anomalous behavior by increasing the loss energy. The EELFS signal above the N_{23} edges decreases more rapidly than that above the M_{45} edges although it occurs in a lower-energy-loss range. This effect should depend on the minimum of the atomic absorption cross section (Cooper minimum) (Refs. 23 and 24) which occurs at almost the same energy.

III. ELECTRONIC PROPERTIES

The main objective of this section is to give an interpretation guideline for the features of a valence REEL spectrum of transition metals within the electronic band-structure framework. The Pd case, then, will be a suitable test of the drawn conclusions. Particular care is devoted to ascertain the kind of correspondence existing between an optical and a REEL spectrum. Anticipating the conclusions, we will show that the same dielectric function $\tilde{\epsilon}(\omega)$ can be used to reproduce the optical as well as the REEL spectrum. Moreover, any structure of the energy-loss spectrum has a simple and direct, although phenomenological, meaning: any peak that occurs in correspondence of a minimum of the joint density of states (JDOS). Instead, optical structures have a rather opposite behavior: The maxima of the JDOS coincide with the structures (maxima) of the optical-absorption spectrum.

A. Assumption and approximations

The response of the solid to the electron or photon probe is described respectively by the longitudinal or transverse dielectric function, and their spatial dispersion $\tilde{\epsilon}(\vec{q}, \omega)$ is generally different. The q -photon momentum exchanged through the electromagnetic interaction is negligible, instead a wide variability range of transfer momentum can occur when the electron-energy-loss experiment is carried out, especially in the reflection mode and without an angle-resolved detection system. In the limit of small transfer momentum q the longitudinal and the transverse dielectric function coincide.²⁵

It has been shown experimentally²⁶ that the maximum q momentum exchanged through the collision of the primary electron with the system by using reflection geometry does not exceed $q = 0.3 \text{ \AA}^{-1}$ and, moreover, that, within this q range, the energy-loss spectroscopy gives the same results as that of optics.

This finding allows us to disregard both the q problem and the differences between the longitudinal and transverse dielectric functions. Consequently, the dipole approximation, generally applied in optics, can be extended also to the inelastic electron scattering.^{11,27}

Within the above dipole scheme and in the Born approximation,^{27,28} the reflected electron provides any information related to the excitation of band electrons. The Bloch electron of the solid is supposed to change its state going to other electronic energy levels and multiple inelastic scattering is not taken into account, since the inelastic

cross section for multiple scattering, which depends on the experimental geometry and on the nature of the medium, should be negligible in REEL experiments on transition metals. The high damping of electron oscillations in transition metals and, moreover, the short electron mean free path in reflection experiments provide that single scattering should be predominant over multiple losses.²⁹

The electron probe interacts strongly with the sample electrons and creates bulk as well as surface longitudinal excitation modes. The electron yield $N(E)$, is therefore, due to the contribution of two terms:^{7,30}

$$N(E) \simeq S \left[-\text{Im} \frac{1}{1 + \tilde{\epsilon}(\omega)} \right] + B \left[-\text{Im} \frac{1}{\tilde{\epsilon}(\omega)} \right], \quad (1)$$

where the first and the second terms arise, respectively, from surface and bulk inelastic scattering.

Within the above approximation ($q \simeq 0$), $\tilde{\epsilon}(\omega)$ is the transverse dielectric function of the solid supposed to be homogeneous up to the solid-vacuum boundary plane. Each contribution can appear in the REEL spectrum in the form of distinct structures, both in energy position and in intensity. Thus any interband transition occurring at $\hbar\omega$ can be associated not only with a bulk inelastic scattering, but also with an inelastic scattering at the boundary plane. The relevance of surface-to-volume scattering at fixed E_p is strictly dependent on the nature of the medium. In a free-electron metal such as aluminum, the main bulk and surface collective excitations are several eV apart.^{26,31} In transition metals, instead, collective electron oscillations are highly damped and the two contributions occur almost at the same energy. In the Pd case, which supports both surface and bulk losses, we can disregard their origin because of the aforementioned energy degeneracy of the two-electron collective modes. The REEL spectra of Fig. 1 are the evidence of how difficult it is to distinguish between the two scattering contributions. In fact, no structure shows a particular evolution with the primary-electron beam E_p although surface effects should be enhanced when $E_p \simeq 70$ –90 eV because of the minimum electron escape depth.³²

Any further attempt requires a careful computational deconvolution of the REEL spectra described in the next section. The obtained results will show that surface and bulk Pd losses are expected to occur too close in energy to be distinctly detected within the experimental energy resolution.

B. Surface versus volume scattering: Phenomenological model

The aim here is to evaluate the relative weight of surface-to-volume scattering in the case of Pd. The coupling of electrons to bulk and surface plasma oscillations for reflection energy-loss measurements has been treated by several authors.^{33,34} The electrons near the surface should excite mainly surface plasmons while those deeper inside have a higher probability of exciting bulk plasmons. Thus, as the electron-beam energy E_p is increased, the greater range of the electrons results in a creation of a

smaller fraction of surface plasmons with respect to bulk plasmons.

It is difficult to compare the amplitude of energy-loss spectra at different primary-beam energies but relative amplitudes within a single spectrum can still be compared if E_p is fixed during each run. In this case the measured electron yield $N(E)$ can be computed by adding properly surface and bulk contributions:¹²

$$N(E) = C_S \left[\int_0^d dz e^{-2z/\cos\theta \Lambda(E_p)} \right] \left[-\text{Im} \frac{1}{1 + \tilde{\epsilon}(\omega)} \right] + C_B \left[\int_d^\infty dz e^{-2z/\cos\theta \Lambda(E_p)} \right] \left[-\text{Im} \frac{1}{\tilde{\epsilon}(\omega)} \right], \quad (2)$$

where θ is the angle between the direction of the impinging electron beam and the normal to the surface ($\theta = 42^\circ$), and $\Lambda(E_p)$ is the electron mean free path³² for primary-beam energy E_p . The energy dependence of Λ is assumed to have a minimum at about 70 eV and increases roughly as \sqrt{E} for higher energies. The coefficients C_S and C_B are assumed to be equal and constant within the same spectrum because they depend essentially on the detection geometry of the spectrometer and on the sample. The variable quantity z is the distance of the elastic scattering site below the surface and $2z/\cos\theta$ is the effective electron path through the sample. The integration limit d is a phenomenological parameter which should delimit a layer of thickness d where surface scattering is predominant.

The model satisfies the boundary conditions for $d=0$ (only bulk scattering) and for $d=\infty$ (only surface scattering). Then the amplitude of surface-to-bulk loss features decreases with increasing beam energy, as expected from electron mean-free-path considerations. Of course, this trend is strongly dependent on d : the smaller is d , the lower or the higher, according to the E_p variability ($E_p \geq 70$ or $E_p \leq 70$ eV), is the beam energy which is necessary to probe only bulk properties. The model has been also tested by Henrich *et al.*¹² who successfully separated bulk and surface features in energy-loss spectra of MgO.

The computed electron yield in the form of $-d^2N(E)/dE^2$ is compared in Fig. 4 with the experimental spectrum taken at $E_p = 150$ eV. The optical data $\tilde{\epsilon}$ have been taken from Weaver *et al.*¹⁰ The inset shows the second derivative of the bulk (solid line) and the surface (dotted line) loss functions obtained from optical data (Ref. 10). The arrow marks the energy position of the most intense feature as determined from the REEL investigation. The fitting parameter d is 1.5 ± 0.2 Å in agreement with the usual assumptions: (i) d is of the order of the wavelength of the impinging electron; (ii) d is determined by the Thomas-Fermi screening³⁵ of the impinging electron at the surface.

The model shows that bulk and surface contributions of Pd differ only in very small shifts of the energies of the loss peaks. Moreover, the plasma loss at about 7 eV is the unique feature which depends only slightly on E_p (Fig. 4, inset). The REEL spectra of Pd confirm this theoretical trend because they do not show any dependence on E_p within the experimental accuracy. The volume contribution to the REEL signal is certainly predominant and the

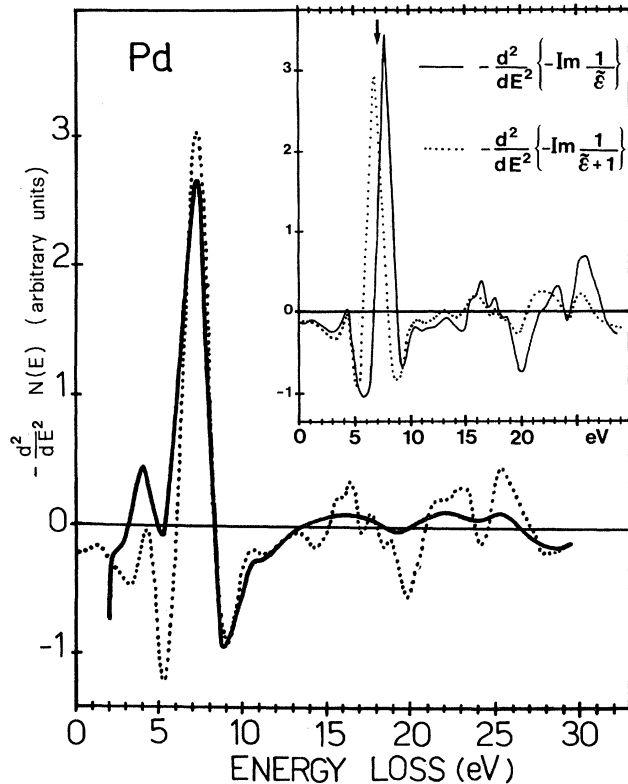


FIG. 4. Comparison between the reflection energy-loss spectrum taken at $E_p=150$ eV (solid line) and the result of the phenomenological model [Eqs. (2)] (dotted line). The inset shows the second derivative of the bulk (solid line) and the surface (dotted line) loss functions obtained from optical data (Ref. 10). The arrow marks the energy position of the main experimental structure.

surface boundary effect, although existing, does not shift the loss peaks. Therefore, the model,¹² although phenomenological, seems to give a proper description of the backscattering mechanism in a REEL experiment. A further and more extensive investigation about the role of bulk and surface contributions in the case of a free-electron-like gas is in progress.²⁶

IV. REEL SPECTRUM AND VALENCE BAND

As far as the energy position of REEL features is taken into account, the superposition of surface and bulk scattering contributions can be disregarded in studying electron properties of Pd. The two contributions are, in fact, energy degenerate within the experimental accuracy.

A. Interpretation scheme

The interpretation guide of valence REEL spectra taken in the second-derivative mode has been already given in a number of papers.^{7,36} Each peak of $-d^2N(E)/dE^2$ is correlated to the probability for an electron to lose the energy ΔE by creating a collective oscillation of Pd valence electrons. On the contrary, the energy localization of individual excitations (optical interband transitions) in the REEL spectra is less straightforward because they occur in the hollow between two adjacent maxima. Within an accuracy of 0.2–0.5 eV which depends on the energy-loss value, they can be localized in the minima and not, certainly, in the maxima of $-(d^2/dE^2)N(E)$ as very often found in the literature.

Table I shows the results of the present work which are in good agreement with transmission¹¹ EEL data and optical loss function computed from optical data¹⁰ confirming that the REEL structures are not artifacts of the second-derivative detection mode. The interpretation of Pd REEL results can be carried out within the band calculations of Laššer and Smith.¹⁹ They also performed a band-to-band decomposition of the imaginary part of the dielectric function $\tilde{\epsilon}$ including momentum matrix element and spin-orbit effects. Figure 5 shows partial $\epsilon_2(i \rightarrow f)$ spectra of Pd for transitions from the initial band i into the final band f . The vertical lines mark the positions of the bulk plasmons as determined from our results (Fig. 1). Each line occurs in a region where the optical absorption is negligible, stressing, once more, that the single-particle and the collective excitations are generally in competition.³⁷

Such a correlation between individual and collective excitations can be also observed in Cu (Ref. 38) and Ni (Ref. 39) partial dielectric functions with even more evidence. Figures 5–7 give strong support to our interpretation scheme of valence REEL spectra in the band-structure

TABLE I. Collective excitations of Pd, Ni, and Cu. The energy-loss values have been determined by averaging on several spectra.

Collective excitations: energy (eV)					
Palladium					
2.7 ± 0.5	4.0 ± 0.3	7.0 ± 0.3	15.0 ± 0.3	21.0 ± 0.3	25.4 ± 0.3
Nickel					
3.2 ± 0.3	6.7 ± 0.3	9.6 ± 0.3	15.0 ± 0.5	19.4 ± 0.3	27.4 ± 0.3
Copper					
4.27 ± 0.3	7.2 ± 0.3	10.3 ± 0.3	15.0 ± 0.3	19.5 ± 0.3	27.5 ± 0.3

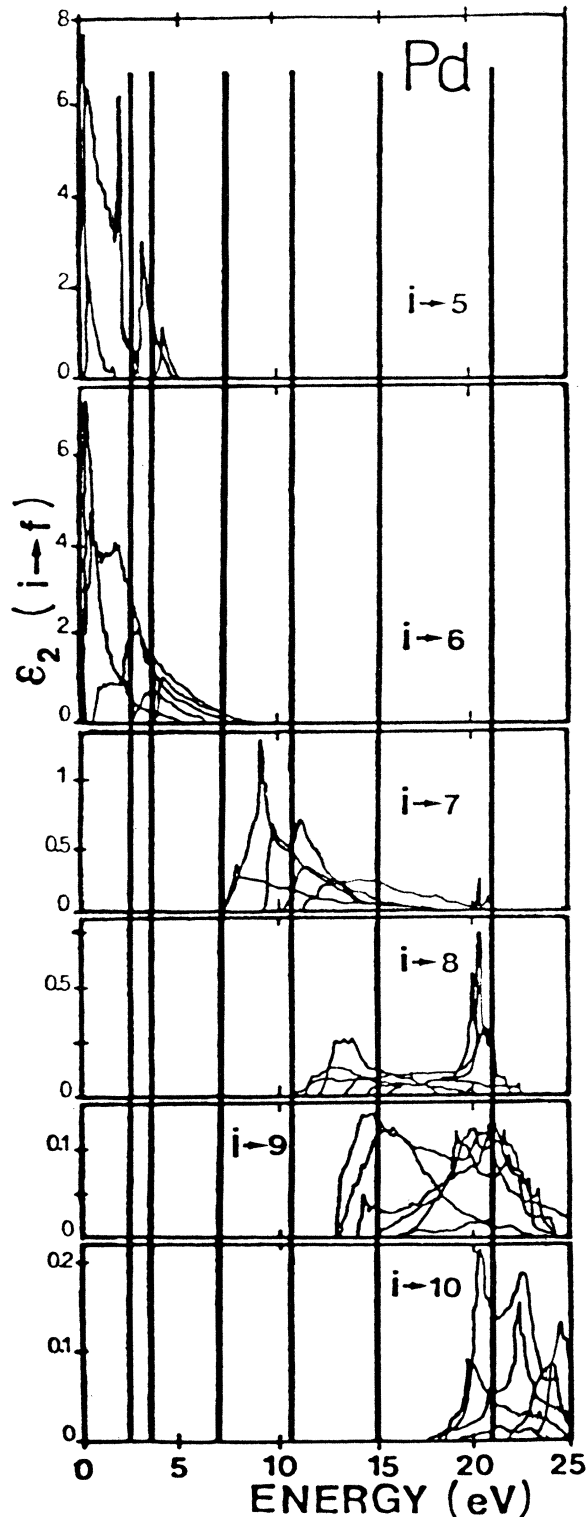


FIG. 5. Partial $\epsilon_2(i \rightarrow f)$ spectra of Pd for transitions from the initial band i into the final band f (Ref. 19). For clarity the initial band indices have not been shown. The contributions of the first two panels should be multiplied by $\frac{1}{7}$.

framework. The energy positions of the bulk plasmons of Cu and Ni are deduced from the REEL spectra of Fig. 8.

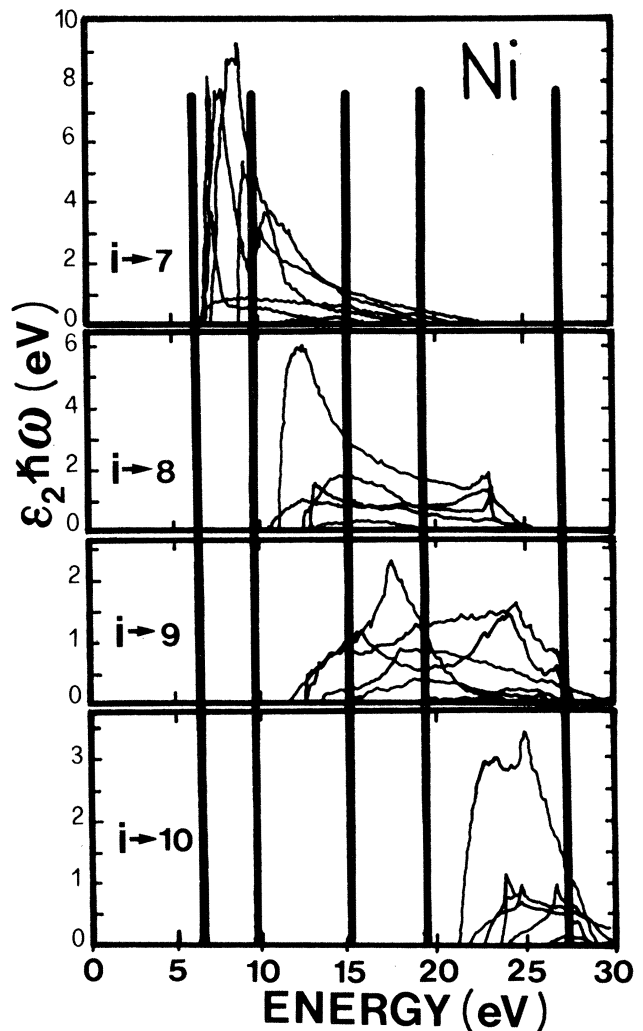


FIG. 6. Band-to-band decompositions for the optical absorption of Ni involving transitions into bands $f=7-10$. The contributions of the first panel should be multiplied by $\frac{1}{2}$.

B. Systematics: Pd, Ni, and Cu

The Pd main plasmon at 7.0 eV which occurs where the optical absorption is almost zero signs the separation between the contribution to ϵ_2 due to transitions into final bands 5,6, and that which is due to transitions involving bands with index $f \geq 7$.¹⁹ Systematic optical studies¹⁰ show a similar minimum in the imaginary part of the dielectric function of all the transition metals. Analogous behavior can be argued in the REEL spectra of Fig. 8 which shows our results for Ni, Cu, and Pd. The bulk plasmons at 6.5 eV in Ni, at 7.2 eV in Cu, and 7.0 eV in Pd all correspond to a pronounced minimum in ϵ_2 which is followed by transitions to final bands with band indices higher than 7. The collective excitations of Ni and Cu are reported in Table I together with the Pd present results. Also Ni and Cu should have a loss feature at about 2 eV but it is too close to the elastic peak to be clearly observed in our spectra.

An intensive comparison between Ni and Cu REEL

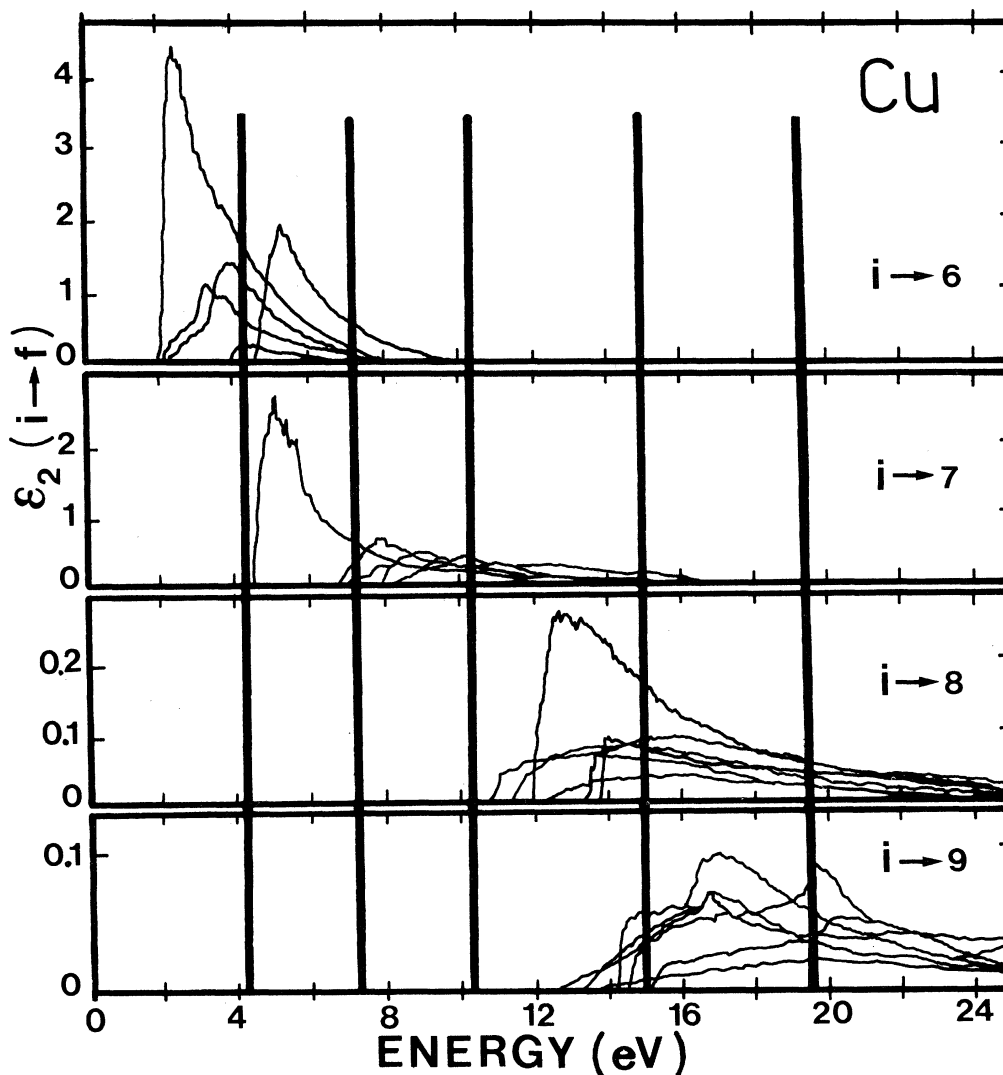


FIG. 7. Partial $\epsilon_2(i \rightarrow f)$ spectra of Cu for transitions from the initial band i to the final band f .

spectra (Fig. 8) shows a one-to-one correspondence among the structures; in particular, on going toward high loss energies, their electronic properties become very similar. All these properties seem to suggest the existence of a REEL line shape which should be typical of the fcc transition metals of the first row rather than of Ni and Cu separately. This statement is supported by a comparative inspection of Ni and Cu electronic band structures (Refs. 38–40) (Fig. 9). Their energy-dispersion lines have an overall similarity since by going from Cu to Ni there occurs essentially an upward shift of band levels lying between -3 and 10 eV around the Fermi level. Therefore, the main differences between Cu and Ni optical absorption can be expected in the low-energy range ($E < 10$ eV) where, indeed, we observe slight changes in the interband transition onsets.

On the contrary, the REEL spectrum of Pd is quite different from Cu and Ni spectra. Nevertheless, it is still possible to find meaningful correlations among them. The energy-band structures shown in Fig. 9 have similar shapes of the energy-dispersion lines but their energy positions are somewhat different. The main differences can be

summarized as follows.

(i) On going from Cu to Ni to Pd, the upward shift of the center of the d band relative to the bottom of Cu conduction band increases, and at X , W , and L symmetry points some energy levels become empty.

(ii) Pd energy levels lying in the $(14-24)$ -eV energy range shift downward at about 4 eV with respect to Cu and Ni with the exception of the levels at X which, instead, remain almost unaffected.

This trend can be observed in the REEL spectra of Pd, Ni, and Cu (Fig. 8). In fact, Pd has more structures than Ni and Cu in the same energy-loss range ($11-35$ eV) since the sinking of the bands 7,8,9,10 along $Q-L-A-\Gamma$ symmetry lines lowers the energy onset of some interband transitions. By using the band-to-band decomposition of ϵ_2 (Refs. 19, 38, and 39) (Figs. 5–7) it is also possible to follow and interpret the systematic trend of REEL structures. For example, the plasmon peak which occurs at 19.5 eV in Cu and Ni vanishes in interband transitions in Pd. In fact, partial $\epsilon_2(i \rightarrow 8)$ and $\epsilon_2(i \rightarrow 10)$ shift downward in Pd and give rise to a two-peak structure at ~ 19 and ~ 23 eV. They correspond to the minima which

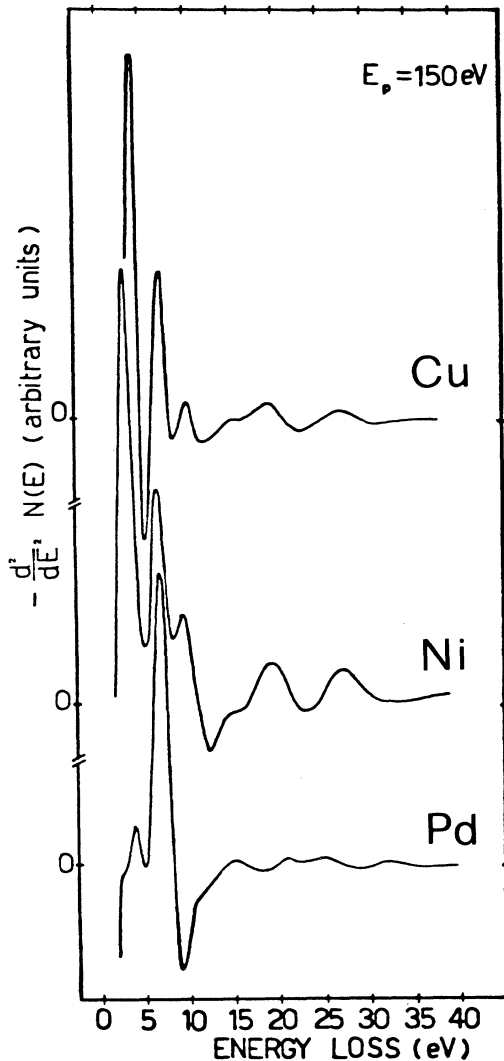


FIG. 8. Electron-energy-loss spectra of Cu, Ni, and Pd taken at the primary-beam energy $E_p = 150$ eV.

occur at the same energy in the REEL spectrum of Pd. Even the plasmonic structure at 21 eV finds its counterpart in the Pd- $\epsilon_2(i \rightarrow 10)$ (Fig. 5). The other big differences among Pd, Ni, and Cu can be observed around 9 eV where the strong optical absorption of Pd corresponds instead to a plasmon in Ni and Cu. The origin of this difference arises along $W-Q-L$ where the energy-band levels 5,6,7 of Pd lie higher than in Ni and Cu. Consequently, the optical absorption which involves these band levels shifts in the ultraviolet with respect to Ni and Cu.

V. REFLECTION EELFS DATA: STRUCTURAL INFORMATION

Optics and valence REEL spectra are strongly related; x-ray and core REEL spectra are also. Even extended fine structures above the core edges are detectable in REEL spectra just as in x-ray absorption spectra. We will show that structural information can be obtained by an EXAFS-like analysis of the REEL signal in the high-energy-loss region.

A. Theoretical aspects and approximations

Quite recently we have shown that structural information can be extracted from the analysis of the oscillations detected in REEL experiments^{5,8,17} above the shallow core levels. Similar fine structures have already been observed in energy-loss transmission^{4,27,41,42} spectra on self-supported thin films and have been interpreted within the Born approximation^{27,28,43} as due to an EXAFS-like effect. Incident and scattered electrons are treated as plane waves, and the inelastic cross section for excitation of an atom containing a core electron in initial state i to a final state f is written within the single-particle model:^{41,43}

$$\frac{d}{dE} \sigma_{if}(E) = \frac{8\pi e^4}{\hbar^2 v^2} \int_{q_{\min}}^{q_{\max}} dq \frac{1}{q^3} |\langle f | e^{i\vec{q} \cdot \vec{r}} | i \rangle|^2, \quad (3)$$

where v is the velocity of incident fast electrons and $\hbar \vec{q}$ is the momentum exchanged in the electron scattering process; q_{\min} and q_{\max} are the limits allowed by the scattering kinematics. For small scattering angles or momentum

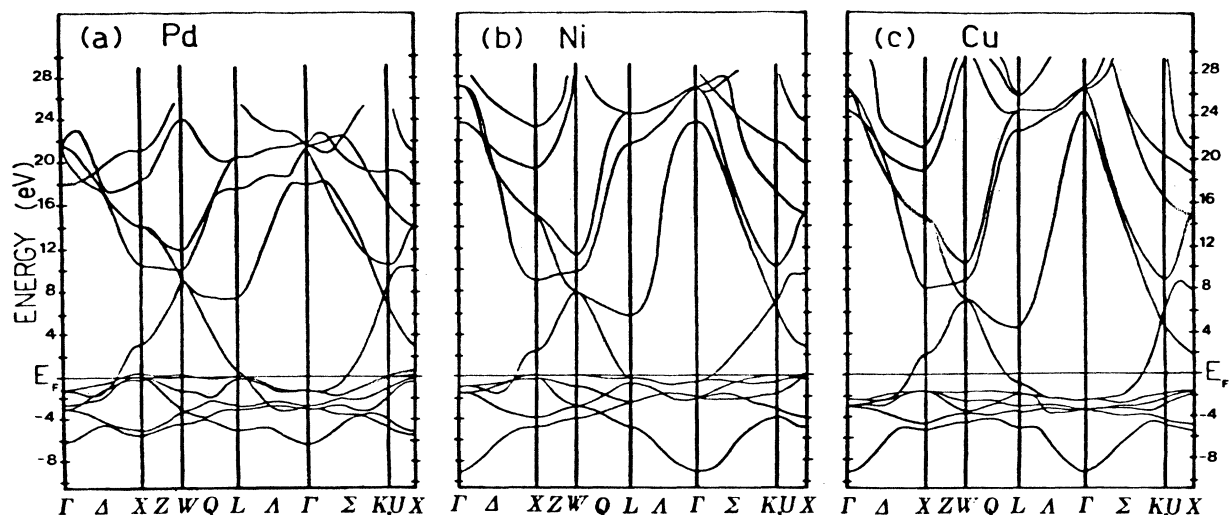


FIG. 9. Electronic band structures of Pd (Ref. 19), Ni (Ref. 40), and Cu (Ref. 38). It should be noted that a compression of Pd energy levels toward the Fermi level with respect to Ni and Cu is shown.

transfers, the cross section $(d/dE)\sigma_{if}(E)$ is given in terms of a dipole matrix element. In this limit, optical selection rules apply and the differential cross section can be turned into the same dipole form of the photoabsorption cross section:^{41,42}

$$\frac{d}{dE}\sigma_{if}(E) = \frac{8\pi e^4}{\hbar^2 v^2} \ln \left[\frac{q_{\max}}{q_{\min}} \right] |\langle f | \vec{\epsilon}_q \cdot \vec{r} | i \rangle|^2. \quad (4)$$

$\vec{\epsilon}_q$ is a unit vector along \vec{q} and plays the same role of the electric field polarization vector $\vec{\epsilon}$ in the x-ray absorption cross section:⁴²

$$\sigma_{if}(\hbar\omega) = \frac{4\pi e^2}{\hbar c} \hbar\omega |\langle f | \vec{\epsilon} \cdot \vec{r} | i \rangle|^2. \quad (5)$$

This conclusion is strictly valid for small momentum transfers and has been found to hold in general. The matrix element [Eq. (3)] depends on the energy loss and the momentum transfer but the inelastic cross section has stronger contributions arising from low- q values as shown by Leapman *et al.*²²

The oscillations detected in x-ray as well as in transmission electron-energy-loss spectra are a consequence of the final-state modulation due to the interference between the outgoing wave function of the excited electron and its backscattered part from the surrounding atoms. The reflection EELFS fine structures can have the same physical origin of the EXAFS signal. On the other hand, the electron-energy-loss yield is related to the dielectric function $\tilde{\epsilon}(E, q) = \epsilon_1 + i\epsilon_2$ through the loss function $\epsilon_2/(\epsilon_1^2 + \epsilon_2^2)$ which, in the range of core-level excitations, becomes proportional to ϵ_2 and consequently to the cross section.

Although we lack an adequate theoretical model, we extend the above-mentioned conclusions on the dipole form of the scattering cross section to the reflection case. Actually the theoretical model of transmission energy-loss experiments should not be adequate to describe the reflection case owing to the low-primary-beam energies ($E_p = 2000$ eV) in comparison with large energy losses ($\Delta E = 500$ eV). Nevertheless, previous investigations^{5,8,17,44} suggest that there is a possible complete identification between transmission and REEL schemes. With these state-of-the-art investigations we are forced to conclude that not only the Born approximation should be considered valid but also that the incident and the scattered electrons could be treated as plane waves if $\Delta E/E \cong \frac{1}{4}$.

We are aware that final-state effects could be observable in the core-level electron-energy-loss spectra and that they should affect, at least in principle, the EELFS oscillations detected above the core edge. Proper investigations at different primary energies (500–2500 eV) do not show any change in the EELFS structures with E_p , in agreement with the suggestions arising from recent results on vanadium,⁴⁵ nickel,⁴⁶ and cobalt.⁴⁷ Thus it remains to be ascertained why, in this primary-beam energy range, possible final-state effects do not influence the EELFS $\tilde{F}(R)$ which, in turn, is very similar to the EXAFS $\tilde{F}(R)$. As we have already pointed out, multiple scattering can be neglected in transition metals also in the core energy range. The EELFS structures of these metals can be considered genuine structural features. On the other hand,

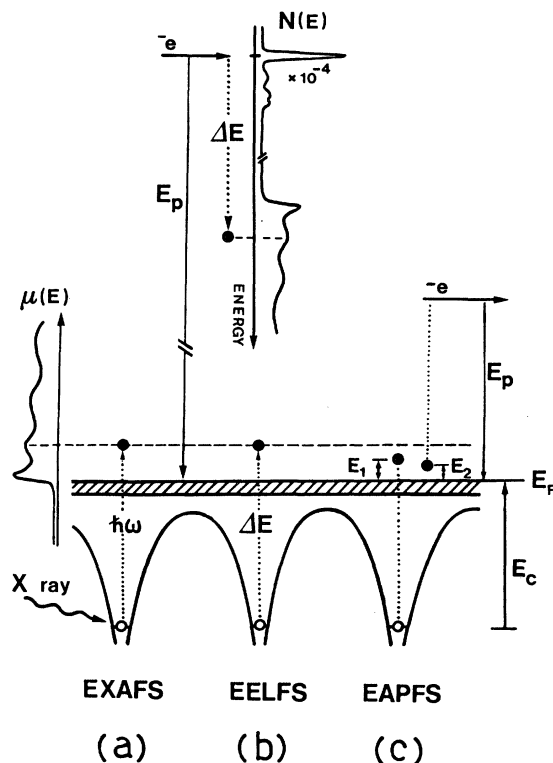


FIG. 10. Schematic comparison between EXAFS (a) and two electron core-level spectroscopies: EELFS (present technique) (b) and EAPFS (c).

the Fourier transform of a multiple plasmonic replica would give a peak lying well above any structural feature (5–10 Å).

The validity of the EXAFS-like formulation should depend also on the spectrometer angle collection since the dipole approximation no longer holds if the momentum transfer is allowed to become large. A CMA detection geometry should average the signal over all the detected momentum transfers enhancing the low- q contribution to the EELFS spectrum. The role of an angle-resolved detection of the EELFS signal is currently being investigated.

The analogies between EXAFS and EELFS spectroscopies are schematically summarized in Fig. 10 where it is shown that the involved final state $|f\rangle$ can be described in the same way. Among core spectroscopies this is a suggestive case of a complete identification of final states, at least within the dipole approximation. For example, the extended appearance potential fine structures^{48–50} can give structural information but the underlying theory⁵¹ requires a more complex description model with two electrons in the final state $|f\rangle$ [Fig. 10(c)]. Moreover, the dipole selection rule cannot be applied in a straightforward way.⁵²

B. EELFS analysis and results

Following the standard procedure for EXAFS analysis^{6,42} we performed the Fourier transform of the EELFS signal $X(E) = -(d^2/dE^2)N(E)$ to obtain

structural information around each Pd excited atom in the form of a pseudo radial distribution function $\tilde{F}(R)$:⁵³

$$\tilde{F}(R) = \frac{1}{\sqrt{2\pi}} \int_{k_{\min}}^{k_{\max}} X(k) e^{-2ikR} dk. \quad (6)$$

Here $k = [(2m/\hbar^2)(E - E_0)]^{1/2}$ is the wave vector⁵⁴ and $E - E_0$ is the kinetic energy of the photoelectron plane wave. E_0 is the core-level threshold.

With this state-of-the-art interpretation, the pseudo radial distribution function $\tilde{F}(R)$ should be limited to the R position of each peak. Since the EELFS signal is recorded in a second-derivative mode, its Fourier transform is proportional to the usual EXAFS pseudo radial function multiplied by R^2 . Thus the higher coordination shells are artificially enhanced. Nevertheless, their positions remain unaffected by this kind of data acquisition. In order to verify this point, many attempts have been made to obtain self-consistent results starting the EXAFS procedure both with $\chi(E)$ and with

$$-d^2\chi(E)/dE^2.$$

The EELFS $\tilde{F}(R)$ results for the N_{23} and M_{45} edges are shown in Fig. 11. Because of the presence of the nearby M_{45} core edges, the integration k range of the N_{23} signal is quite short ($2-7 \text{ \AA}^{-1}$) and, consequently, the $\tilde{F}(R)$ function is rather broad. Instead, the radial distribution

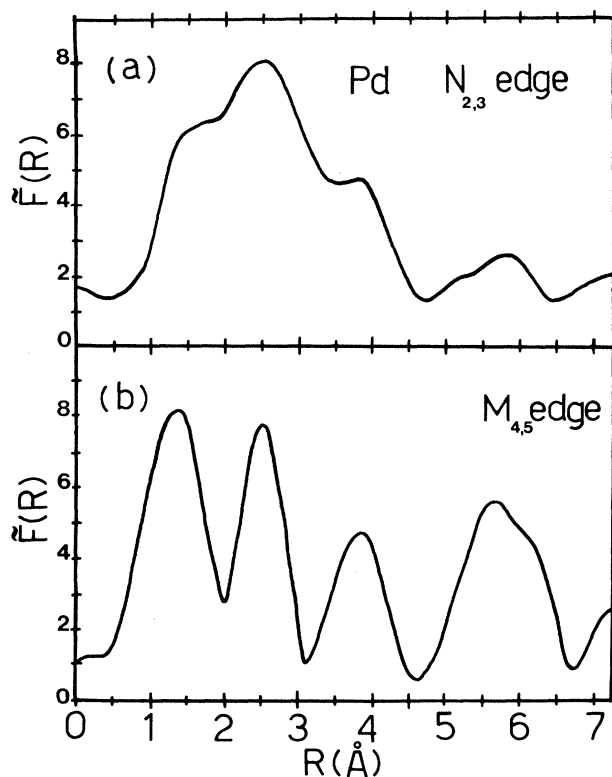


FIG. 11. Pd pseudo radial distribution function obtained from EELFS oscillations above the N_{23} edge (a) and the M_{45} edge (b).

function for the M_{45} case shows more resolved structures but a one-to-one correspondence between peaks in N_{23} and M_{45} $\tilde{F}(R)$ is still clearly seen. Although each peak of the $\tilde{F}(R)$ function should be related to the neighbors' shell through the EXAFS phase shift, no phase-shift effect can be detected on going from the N_{23} to the M_{45} edges. A number of attempts have been performed to rule out the chance that this result could be an artifact of the short k range of integration. An arbitrary narrowing of the k range for the M_{45} case does not shift at all the peaks of $\tilde{F}(R)$ but results in more broad structures.

The main peak at $2.50 \pm 0.05 \text{ \AA}$ is related to the nearest-neighbor shell. Unfortunately, no deeper interpretation can be attempted because theoretical phase shifts for core levels shallower than L_{23} do not exist.⁵⁵ Recently, Ekardt and Tran Thoi⁵⁶ have justified the use of the L_{23} phase shifts in the interpretation of the M_{23} EELFS oscillations, but there is no evidence about a possible extension of their conclusions to the N_{23} and M_{45} cases.

The low-lying structure at $\sim 1.5 \text{ \AA}$ of $\tilde{F}(R)$ has no interpretation in terms of neighbor shells. Its main origin is due to a Ramsauer-Townsend resonance in the Pd back-

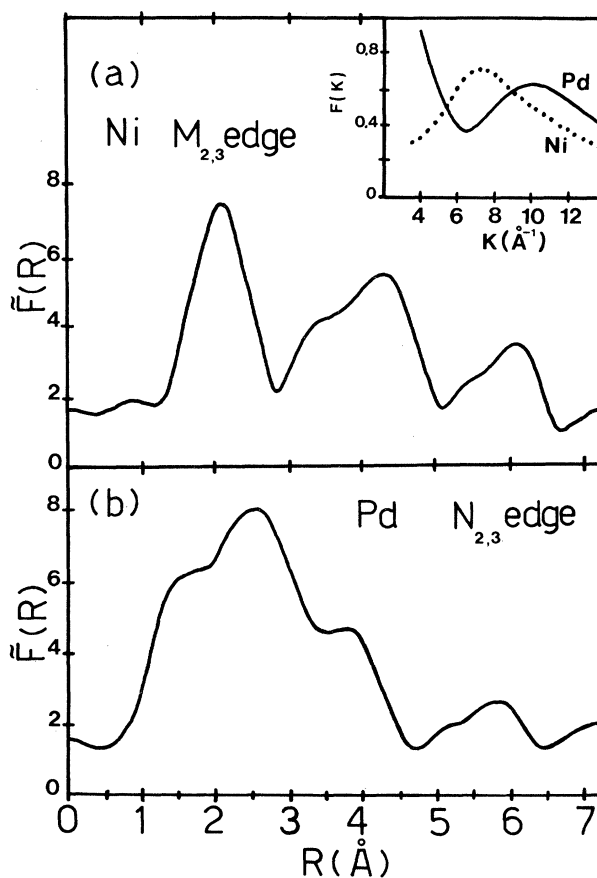


FIG. 12. EELFS $\tilde{F}(R)$ obtained from M_{23} -Ni oscillations (a) (Ref. 5) and from N_{23} -Pd oscillations (b). The inset shows the backscattering amplitude of Ni and Pd computed by Teo and Lee (Ref. 55).

scattering amplitude which is, then, typical for the heavy elements.⁵⁵ The amplitude modulation which is present in Pd and not, for example, in Ni gives rise to a double structure in the $\tilde{F}(R)$ of Pd. As it can be seen in Fig. 12, the Ni pseudo radial distribution function obtained from EELFS oscillations above the M_{23} edges has only a peak in the low radial range (1–3 Å) to be compared with the N_{23} pseudo radial distribution function of Pd. This effect of backscattering amplitude, however, has already been observed in the EXAFS spectra of gold⁵⁷ and confirms further the reliability of the EELFS spectroscopy.

Of course, in the case of the M_{45} core level, the low-lying structure of $\tilde{F}(R)$ is also affected by the superposition with the oscillations above the N_{23} edges. This could be the main origin of the different intensity of the structure at 1.4 Å in N_{23} and M_{45} $\tilde{F}(R)$. Instead, no artifact effect⁴¹ should be ascribed to the superposition of the oscillations above the M_4 and M_5 edges. A model calculation which reproduces the EELFS spectrum with the statistical weights of the two core levels does not show any dependence on their spin-orbit splitting⁵⁸ (~6 eV).

Analogous interpretation problems arise from L_{23} EXAFS studies of Pd since also in this case the narrow K -range integration (2–8 Å) is due to the superposition of L_2 and L_3 EXAFS oscillations. The L_{23} EXAFS- $\tilde{F}(R)$ is very similar to the N_{23} EELFS- $\tilde{F}(R)$ as it should be because of the same initial angular momentum.

More definitive conclusions on the use of EELFS spectroscopy as a standard structural technique awaits for EXAFS and EELFS measurements on the same core level and for the signal analysis over the same k -integration range. The Ti case should be quite proper since the shallow L_{23} edge can be excited by the electron probe and the results can be compared with the existing EXAFS data.⁵⁹ A work in this sense is in progress.⁶⁰

V. CONCLUSIONS

Valence REEL spectra of Pd are interpreted within a band-structure framework in a way that is not always acknowledged. This method should mark the passage from a qualitative to a quantitative use of REEL spectroscopy.

Collective excitations localize the minima of JDOS and should be considered a powerful tool for testing theoretical band-structure calculations just as with optical excitations. The momentum transfer problem of reflection REEL spectroscopy seems to be generally negligible since the comparison with optical data gives a one-to-one correspondence between REEL and optics results. REEL spectra find a counterpart in optical data even in the tiny features.

Core REEL spectra show extended oscillations above the core edges also when the experiment is carried out in reflection geometry. Their interpretation has been performed within the EXAFS theory because of the lack of a proper theoretical model.

Although a number of theoretical problems are still open, for example, phase shifts for core edges shallower than L are not available and the contribution of multipole terms to the EELFS matrix element has not yet been evaluated, nevertheless the analysis of the EELFS oscillations of a REEL spectrum seems to be very suitable for structural investigations.

Previous experimental works on Cu and Ni and the present work on Pd are the best confirmation of the validity of the technique for valence as well as core studies. REEL spectroscopy assumes then an important and promising role in the experimental works requiring samples prepared *in situ*. In fact, in the same UHV chamber it can be used as a characterization technique such as Auger and low-energy electron diffraction, obtaining electronic and structural information.

¹H. Froitzheim, in *Electron Spectroscopy for Surface Analysis*, Vol. 4 of *Topics in Current Physics*, edited by H. Ibach (Springer, New York, 1977).

²C. Kunz, in *Optical Properties of Solids: New Developments*, edited by B. O. Seraphin (North-Holland, Amsterdam, 1976), Chap. 10.

³H. Raether, in *Excitations of Plasmon and Interband Transitions by Electrons*, Vol. 88 of *Springer Tracts in Modern Physics*, edited by H. Raether (Springer, New York, 1980).

⁴J. J. Ritsko, P. C. Gibbons, and S. E. Schnatterly, *Phys. Rev. Lett.* **32**, 671 (1974).

⁵M. De Crescenzi, L. Papagno, G. Chiarello, R. Scarmozzino, E. Colavita, R. Rosei, and S. Mobilio, *Solid State Commun.* **40**, 613 (1981).

⁶P. A. Lee, P. H. Citrin, P. Eisenberger, and B. M. Kincaid, *Rev. Mod. Phys.* **53**, 671 (1981).

⁷E. Colavita, M. De Crescenzi, L. Papagno, R. Scarmozzino, L. S. Caputi, R. Rosei, and E. Tosatti, *Phys. Rev. B* **25**, 2490 (1982).

⁸L. Papagno, M. De Crescenzi, G. Chiarello, E. Colavita, R. Scarmozzino, L. S. Caputi, and R. Rosei, *Surf. Sci.* **117**, 525 (1982).

⁹J. H. Weaver, *Phys. Rev. B* **11**, 1416 (1975).

¹⁰J. H. Weaver, C. Krafka, D. W. Lynch, and E. E. Kock, in *Optical Properties of Metals in Physik Dateu*, edited by Fach Information (Zentrum, Karesruha, 1981), Vols. I and II.

¹¹J. Daniels, C. von Feustenberg, H. Raether, and K. Zeppenfeld, *Optical Constants of Solids by Electron Spectroscopy*, Vol. 54 of *Springer Tracts in Modern Physics* (Springer, New York, 1970).

¹²V. E. Henrich, G. Dresselhaus, and H. J. Zeiger, *Phys. Rev. B* **22**, 4764 (1980).

¹³U. Del Pennino, P. Sassaroli, S. Valeri, and S. Nannarone, *Surf. Sci.* **122**, 307 (1982).

¹⁴J. L. Freeouf, G. W. Rubloff, P. S. Ho, and T. S. Kuan, *Phys. Rev. Lett.* **43**, 1836 (1979).

¹⁵S. Nannarone, C. Rinaldi, and L. Sorba, *Surf. Sci.* (to be published).

¹⁶M. De Crescenzi, G. Chiarello, E. Colavita, and R. Rosei, *Solid State Commun.* **44**, 845 (1982).

¹⁷M. De Crescenzi, F. Antonangeli, C. Bellini, and R. Rosei, *Phys. Rev. Lett.* **50**, 1949 (1983).

¹⁸R. Rosei, M. De Crescenzi, F. Sette, C. Quaresima, A. Savoia, and P. Perfetti, *Phys. Rev. B* **28**, 1161 (1983).

¹⁹R. Lassér and N. V. Smith, *Phys. Rev. B* **25**, 806 (1982).

²⁰K. Okuno, T. Ito, M. Iwami, and A. Hiraki, *Solid State Com-*

- mun. **44**, 209 (1982).
- ²¹J. E. Müller, O. Jepsen, and J. W. Wilkins, *Solid State Commun.* **45**, 365 (1982).
- ²²R. D. Leapman, P. Rez, and D. F. Mayers, *J. Chem. Phys.* **72**, 1232 (1980).
- ²³J. W. Cooper, *Phys. Rev.* **128**, 681 (1962).
- ²⁴S. T. Manson and J. W. Cooper, *Phys. Rev.* **165**, 126 (1968).
- ²⁵E. Tosatti, *Nuovo Cimento* **63B**, 54 (1969).
- ²⁶S. Plutino, E. Colavita, G. Chiarello, and M. De Crescenzi (unpublished).
- ²⁷S. E. Schnatterly, *Solid State Phys.* **34**, 275 (1979).
- ²⁸D. Pines, *Elementary Excitations in Solids* (Benjamin, New York, 1977).
- ²⁹We observed multiple plasmon replica only in the REEL spectra of free-electron-like metals. In transition metals, instead, we have never detected multiple loss features over a wide range of the primary-beam energy.
- ³⁰W. K. Schubert and E. L. Wolf, *Phys. Rev. B* **20**, 1855 (1980).
- ³¹P. M. Th. M. Van Attekum and J. M. Trooster, *Phys. Rev. B* **18**, 3872 (1978).
- ³²I. Lindau and W. E. Spicer, *J. Electron Spectrosc. Relat. Phenom.* **3**, 409 (1974).
- ³³R. H. Ritchie, *Phys. Rev.* **106**, 874 (1957).
- ³⁴P. J. Fiebelman, *Surf. Sci.* **36**, 558 (1973).
- ³⁵J. M. Ziman, *Principles of Theory of Solids* (University Press, Cambridge, 1970).
- ³⁶M. De Crescenzi, E. Colavita, L. Papagno, G. Chiarello, R. Scarmozzino, L. S. Caputi, and R. Rosei, *J. Phys. F* **13**, 895 (1983).
- ³⁷L. S. Caputi, E. Colavita, M. De Crescenzi, S. Modesti, L. Papagno, R. Scarmozzino, R. Rosei, and E. Tosatti, *Solid State Commun.* **39**, 117 (1981).
- ³⁸R. Lassër, N. V. Smith, and R. L. Benbow, *Phys. Rev. B* **24**, 1895 (1981).
- ³⁹N. V. Smith, R. Lassër, and S. Chiang, *Phys. Rev. B* **25**, 793 (1982).
- ⁴⁰F. Smulowicz and D. M. Pease, *Phys. Rev. B* **17**, 3341 (1978).
- ⁴¹R. D. Leapman, L. A. Grunes, and P. L. Fejes, *Phys. Rev. B* **26**, 614 (1982).
- ⁴²*EXAFS Spectroscopy*, edited by B. K. Teo and D. C. Joy (Plenum, New York, 1980).
- ⁴³L. Landau and E. Lifchitz, *Mécanique Quantique, Théorie Nonrelativistique* (Editions Mir, Moscow, 1966).
- ⁴⁴M. De Crescenzi, F. Antonangeli, C. Bellini, and R. Rosei, *Solid State Commun.* **46**, 875 (1983).
- ⁴⁵C. J. Powell and N. E. Erickson, *Phys. Rev. Lett.* **51**, 61 (1983).
- ⁴⁶T. Jach and C. J. Powell, *Solid State Commun.* **40**, 967 (1981).
- ⁴⁷S. Modesti (private communication).
- ⁴⁸R. L. Park and J. E. Houston, *Rev. Sci. Instrum.* **41**, 1810 (1970).
- ⁴⁹M. L. den Boer, T. L. Einstein, W. T. Clam, R. L. Park, L. D. Roelofs, and G. E. Laramore, *Phys. Rev. Lett.* **44**, 496 (1980).
- ⁵⁰G. Ertl and J. Küppers, *Low Energy Electrons and Surface Chemistry* (Verlag Chemie, 1974).
- ⁵¹G. E. Laramore, *Phys. Rev. B* **18**, 5254 (1978).
- ⁵²P. O. Nilsson and J. Kanski, *Surf. Sci.* **37**, 700 (1973).
- ⁵³The term pseudo reminds us that each peak of the $\tilde{F}(R)$ function must be properly shifted by the EXAFS phase in order to obtain the crystallographic radius of the neighbor shell.
- ⁵⁴The wave vector k could be affected by a constant (inner potential) because the kinetic energy of the electron inside and outside the solid is different. However, we used the measured value of E_0 .
- ⁵⁵B. K. Teo and P. A. Lee, *J. Am. Chem. Soc.* **101**, 2815 (1979).
- ⁵⁶W. E. Ekardt and D. B. Tran Thoai, *Solid State Commun.* **45**, 1083 (1983).
- ⁵⁷P. Rabe, G. Tolkiehn, and A. Werner, *J. Phys. C* **12**, 899 (1979).
- ⁵⁸J. A. Bearden and A. F. Burr, *Rev. Mod. Phys.* **39**, 125 (1967).
- ⁵⁹D. Denley, R. S. Williams, P. Perfetti, D. A. Shirley, and J. Stohr, *Phys. Rev. B* **19**, 1762 (1979).
- ⁶⁰M. De Crescenzi, G. Chiarello, E. Colavita, R. Meweo, *Phys. Rev. B* **29**, 3730 (1984).